Long non-coding RNA OIP5-AS1 aggravates acute lung injury through promoting inflammation and cell apoptosis via regulating miR-26a-5p/TLR4 axis

Qingsong Sun
The Affiliated Huaian No.1 People's Hospital of Nanjing Medical University
Man Luo
The Affiliated Huaian No.1 People's Hospital of Nanjing Medical University
Zhiwei Gao
The Affiliated Huaian No.1 People's Hospital of Nanjing Medical University
Xiang Han
The Affiliated Huaian No.1 People's Hospital of Nanjing Medical University
Weiqin Wu
The Affiliated Huaian No.1 People's Hospital of Nanjing Medical University
Hongmei Zhao (hayyzhhm@hotmail.com)
The Affiliated Huaian No.1 People's Hospital of Nanjing Medical University

Research Article

Keywords: OIP5-AS1, miR-26a-5p, TLR4, acute lung injury

Posted Date: March 3rd, 2021

DOI: https://doi.org/10.21203/rs.3.rs-228408/v1

Version of Record: A version of this preprint was published at BMC Pulmonary Medicine on July 14th, 2021. See the published version at https://doi.org/10.1186/s12890-021-01589-1.

Abstract

Background: Acute lung injury (ALI) is a pulmonary disorder that leads to acute failure of respiration and thereby results in a high mortality worldwide. Increasing studies have verified that TLR4 is a promoter in ALI, however, the underlying upstream mechanisms of TLR4 was still rarely investigated.

Methods: Lipopolysaccharide (LPS) was used to induce cell model and animal model. A wide range of experiments including RT-qPCR, Western blot, ELISA, flow cytometry, H&E staining, RIP, luciferase activity and caspase-3 activity were carried out to figure out the expression status, specific role and potential upstream mechanism of TLR4.

Result: RT-qPCR identified that TLR4 expression was upregulated in ALI mice and LPS-induced WI-38 cells. Moreover, miR-26a-5p was confirmed to target TLR4 according to luciferase reporter assay. Besides, miR-26a-5p overexpression decreased the contents of proinflammatory factors (TNF-α and IL-1β) and restrained cell apoptosis, while upregulation of TLR4 reversed these effects of miR-26a-5p mimics, implying that miR-26a-5p alleviated ALI through regulating TLR4. Afterwards, OIP5-AS1 was identified to bind with miR-26a-5p by RNA immunoprecipitation (RIP) and luciferase reporter assay. Functionally, OIP5-AS1 upregulation accelerated the inflammation injuries and miR-26a-5p overexpression counteracted the influence of OIP5-AS1 upregulation on proinflammatory factors and cell apoptosis.

Conclusion: OIP5-AS1 accelerated ALI through regulating miR-26a-5p/TLR4 axis in ALI mice and LPS-induced cells, which indicates a promising insight into diagnostics and therapeutics in ALI.

Introduction

Acute lung injury (ALI), a category of severe respiratory disorder, is characterized by heterogeneous pathologic factors (Ho, Mei, & Stewart, 2015; Mahadeo et al., 2020). With a high morbidity and mortality, ALI has posed a huge threat to human life and health globally (Favarin, de Oliveira, de Oliveira, & Rogerio Ade, 2013; Sadowitz, Roy, Gatto, Habashi, & Nieman, 2011). Previous studies have verified that ALI was closely associated with acute inflammatory response (Ali, Abdel-Hamid, & Toni, 2018; J. Lou et al., 2019; Shin et al., 2017; Song et al., 2019), and large numbers of studies have attempted to find an effective therapy for ALI, whereas the mortality rate of ALI patients is still sorrowfully high (Guo & Ward, 2007; Sadowitz et al., 2011). Therefore, it is crucial to explore the potential molecular mechanisms underlying inflammation response for the improvement of ALI clinical therapy.

Long noncoding RNAs (lncRNAs) are noncoding RNAs with longer than 200 nucleotides that participate in many biological and physiological processes (Vishnubalaji, Shaath, Elango, & Alajez, 2020; Zhao et al., 2020). It is widely accepted that lncRNAs are able to act as miRNA “sponges” to compete with mRNAs for miRNAs with shared miRNAs responses elements (MREs) and can regulate miRNAs (W. Lou, Ding, & Fu, 2020; X. Z. Zhang, Liu, & Chen, 2020; Zhao et al., 2020).

Importantly, it is reported that this ceRNA regulatory network is broadly implicated in multiple pathogeneses including ALI (Abdollahzadeh et al., 2019; Jiang et al., 2020; Zhou, Zhu, Gao, & Zhang, 2019). For instance, the knockdown of lncRNA X-inactive specific transcript mitigates primary graft dysfunction through sponging miR-21 and targeting IL-12A following lung transplantation (Y. Zhang, Zhu, Gao, & Zhou, 2019). Additionally, CASC2 was identified to inhibit lung epithelial cell apoptosis by targeting miR-144-3p/AQP1 axis, and thereby improve ALI (H. Li, Shi, Gao, Ma, & Sun, 2018). Recently, lncRNA OPA-interacting protein 5 antisense transcript 1 (OIP5-AS1) has been reported to involve in diverse pathogeneses including tumors (Chen et al., 2019; Ma et al., 2020), myocardial ischaemia/reperfusion (MI/R) injury (Niu et al., 2020), and osteoarthritis (Zhi et al., 2020). Moreover, OIP5-AS1 was proven to regulate cell injury and inflammatory response in atherosclerosis and rheumatoid arthritis (Qing & Liu, 2020; Ren et al., 2020). However, the role of OIP5-AS1 remained to be studied in ALI.

MicroRNAs (miRNAs), another group of non-coding RNAs, comprised about 22 nucleotides and they can post-transcriptionally regulate gene expression (Bartel, 2004; Machackova et al., 2016). For example, miR-126 blocks the development of coronary atherosclerosis in the mice via targeting S1PR2 (J. L. Fan, Zhang, & Bo, 2020). Besides, miR-38 protects endothelial cell against inflammatory damage in coronary heart disease via targeting CXCR4 (Y. Li et al., 2020). Previously, miR-26a-5p was confirmed to be increased in rheumatoid arthritis patients' synovial tissues and elevates the invasion ability of synovial fibroblasts via targeting Smad 1 (W. Zhang, Chen, Jiang, & Shen, 2018). MiR-26a-5p negatively modulates the development of neuropathic pain in CCI rat models via targeting MAPK6 (Y. Zhang et al., 2018). Nevertheless, the potential target mRNA(s) of miR-26a-5p remain(s) to be elucidated in ALI.

Accumulating studies has proved that (toll like receptor 4) TLR4 is a key regulator of inflammatory response(Zuniga et al., 2017; Zusso et al., 2019). For example, TLR4 aggravates the inflammation and apoptosis of retinal ganglion cells in high glucose (Hu, Yang, & Ai, 2017). In addition, TLR4 silence decreases the inflammation which further prevents the kidney damage and the development of fibrosis in cyclosporine nephrotoxicity (Gonzalez-Guerrero et al., 2017). Howver, the role of TLR4 deserves a further exploration in ALI.

In this study, we established animal and cell models of ALI by LPS treatment to exact role as well as the regulatory function of OIP5-AS1 in ALI. We found out that OIP5-AS1 aggravated ALI development through promoting inflammation and cell apoptosis via regulating miR-26a-5p/TLR4 axis. Our findings might offer a promising approach for ALI treatment.

Materials And Methods

ALI mice model

Total 64 BALB/c mice were kept in a room with a temperature of 25℃ in a light/dark cycle of 12 h/12 h. Then all the mice were divided into two groups randomly: Sham group (n=8) and ALI group (n=54). For construction of the ALI mice model, 10 μg lipopolysaccharide (LPS; Sigma-Aldrich Inc., USA) in 50 μL of phosphate buffer saline (PBS; Sigma-Aldrich) was intratracheally instilled while the mice in the sham

group were injected with an equivalent volume of PBS (Sigma-Aldrich). After 6 h, the mice were sacrificed, and lung tissues were collected for RT-qPCR, western blot and HE staining assays. All experimental procedures were based on the National Institutes of Health Guidelines for the Care and Use of Laboratory Animals and approved by the Ethics Committee of The Affiliated Huaian No.1 People's Hospital of Nanjing Medical University. All methods were conducted in accordance with the ARRIVE guidelines (https://arriveguidelines.org).

Wet/dry ratio of the lungs

The examination of lung W/D weight ratio was used to evaluate pulmonary edema. After the killing of mice, the fresh lung tissue was weighed and recorded, following the drying at 180 °C in an oven for 24 h to examine dry weight.

Histological analysis

The mouse lung tissue samples were immobilized with 10% formalin was for one day. After embedding in the paraffin, the tissues were sliced into 5 μM pieces. Furthermore, the tissue pieces were dealt with haematoxylin-eosin (H&E) staining and observed with a light microscope (Nikon, Japan). The following standards were used to score the lung injury, 0: no damage or minimal damage; 1: mild damage; 2: moderate damage; 3: severe damage; 4: diffuse injury.

Adeno-Associated Virus injection

Mice were received with a tail vein injection of an adeno-associated virus 6 (AAV6) system as described previously. AAV carrying miR-26a-5p (or the NC Mock), TLR4 (or NC vector) and OIP5-AS1 (or NC vector) were synthesized by Hanheng Biotechnology Co., Ltd. (Shanghai, China).

Cell culture and transfection

The Human embryonic lung cells WI-38 and mice lung epithelial TC-1 cells (Cell Bank of Type Culture Collection of Chinese Academy of Sciences, Shanghai, China) were maintained in DMEM (Sigma-Aldrich) containing 5% FBS (Gibco, USA), 100 U/mL penicillin and 100 μg/mL streptomycin at 37℃ in a 5% CO_2 atmosphere. For cell transfection, miR-26a-5p mimics, pcDNA3.1/OIP5-AS1, pcDNA3.1/TLR4 with corresponding negative controls were transfected into WI-38 and TC-1 cells by Lipofectamine 2000 (Invitrogen, USA). After 48 h transfection, the cells were harvested and utilized for further use. Vectors were obtained from Genepharma (Shanghai, China).

Quantitative real-time polymerase chain reaction (RT-qPCR)

Total RNA was extracted from WI-38 and TC-1 cells or tissues with Trizol reagent (Invitrogen; Thermo Fisher Scientific, Inc. USA). For miRNA analysis, the extracted RNA was reversely transcribed into complementary DNA (cDNA) with a TaqMan MicroRNA Reverse Transcription Kit (Invitrogen). For lncRNAs and mRNAs analysis, RNA was reversely transcribed into cDNAs by use of the Oligo dT primer (T

(Invitrogen)). PCR reactions were conducted on an ABI 7500 Real-Time PCR System (Applied Biosciences, USA). The gene levels were determined by employing the $2^{-\Delta\Delta Ct}$ method standardized to GAPDH or U6. The primers used for RT-qPCR (Bioneer Technology, CA) were as follows:

hBax

qPCR: F：TCATGGGCTGGACATTGGAC,

R：GCGTCCCAAAGTAGGAGAGG;

mBax

qPCR: F：CTGGATCCAAGACCAGGGTG,

R：CTTCCAGATGGTGAGCGAGG;

hBcl-2

qPCR: F：TTTGAGTTCGGTGGGGTCAT,

R：AGAAATCAAACAGAGGCCGCA;

mBcl-2

qPCR: F：AACATCGCCCTGTGGATGAC,

R：TGCACCCAGAGTGATGCAG;

hIL-1β

qPCR: F：TGAGCTCGCCAGTGAAATGA,

R：CATGGCCACAACAACTGACG;

mIL-1β

qPCR: F：TGCCACCTTTTGACAGTGATG,

R：TGATGTGCTGCTGCGAGATT;

hTNF-α

qPCR: F：CTGGGGCCTACAGCTTTGAT,

R：GGCCTAAGGTCCACTTGTGT;

mTNF-α

qPCR: F□ACTGAACTTCGGGGTGATCG,

R□GTTTGCTACGACGTGGGCTA;

hGAPDH

qPCR: F□ GCTCTCTGCTCCTCCTGTTC,

R□GACTCCGACCTTCACCTTCC;

mGAPDH

qPCR: F□ GGAGAGTGTTTCCTCGTCCC,

R□ATGAAGGGGTCGTTGATGGC;

hTLR4

qPCR: F□ GACGGTGATAGCGAGCCAC,

R□TTAGGAACCACCTCCACGCAG;

mTLR4

qPCR: F□CCTGTGGACAAGGTCAGCAA,

R□CTCGGCACTTAGCACTGTCA;

miR-26a-5p: UUCAAGUAAUCCAGGAUAGGCU;

Mock: UCUCCGAACGUGUCACGUU;

Mimic: UUCAAGUAAUCCAGGAUAGGCU;

Inhibitor: AGCCUAUCGAUAUACUUGAA;

qPCR: F□TTCAAGTAATCCAGGA,

R□GTGCAGGGTCCGAGGT;

U6

qPCR: F□CTCGCTTCGGCAGCACA,

R□AACGCTTCACGAATTTGCGT;

RNA immunoprecipitation (RIP) assay

The RIP assay was conducted in a Magna RIP RNA-Binding Protein Immunoprecipitation Kit (Millipore, USA). Briefly, cell lysate of WI-38 or TC-1 cell was centrifuged for 30 min at 12,000 × *g* and the supernatant were collected. Ago2 antibody (Otwo Biotech, Shenzhen, China) or IgG (Sigma, USA) were respectively cultured with protein G-agarose beads for 2 h at 4℃ and then cell lysate supernatant was filled in and cultured overnight at 4℃. RNA was isolated from magnetic beads with TRIzol reagent (Invitrogen) and RT-qPCR was used to detected OIP5-AS1 and miR-26a-5p in the precipitates.

Western blot analysis

Tissues and cells were harvested and lysed by use of protein lysis buffer (Bio-Rad Laboratories). Then equal amount of proteins samples was separated on SDS-12% PAGE followed by transferring onto polyvinylidene difluoride (PVDF) membranes. Blocked by 5% skimmed milk for 1 h at indoor temperature, and cultured with the primary antibodies against TLR4 (ab22048; Abcam, UK), Bax (ab32503; Abcam), Bcl-2 (ab32124; Abcam) and GAPDH (ab181602; Abcam) were incubated at 4°C for 24h. Washed by utilizing TBS (Bio-Rad Laboratories), the membranes were then cultured with HRP-conjugated secondary antibodies at room temperature for 2 h. At last, the protein bands were assessed via an ECL kit (Amersham Biosciences) and the intensity was analyzed by employing ImageJ software.

Luciferase reporter assay

The wild type luciferase reporter vectors of TLR4 (pmirGLO-TLR4 -WT) or OIP5-AS1 (pmirGLO-OIP5-AS1-WT) containing the potential targeted sites of miR-26a-5p were established by Genepharma (Shanghai, China). The mutant TLR4 (or pmirGLO-TLR4 -Mut) or OIP5-AS1 (pmirGLO-OIP5-AS1-Mut) was also constructed. Afterwards, the vectors were co-transfected with miR-26a-5p, anti-miR-26a-5p or Mock into TC-1 and WI-38 cells by use of Lipofectamine 2000 (Invitrogen), separately. After 48 h, the relative luciferase activities were detected with luciferase reporter assay system (Promega, USA).

Flow cytometry assay

The apoptosis rate of TC-1 and WI-38 cells was evaluated through Annexin V fluorescein isothiocyanate/propidium iodide (Annexin V-FITC/PI) apoptosis assay kit (Invitrogen) following previous procedures (Rieger, Nelson, Konowalchuk, & Barreda, 2011). In short, TC-1 and WI-38 cells treated with LPS after transfection and then subjected to staining with Annexin V-FITC and PI for 25 min in the dark. Afterwards, the flow cytometry (FACS 420, BD Biosciences, USA) was used to analyze apoptotic cells. Percentage of apoptosis rate was calculated as apoptotic cells/total cells × 100%.

The caspase-3 activity detection

The caspase-3 activity in lung tissues was measured by caspase-3 activity kit (Beyotime). The tissues were isolated, prepared and lysed in cell lysis buffer. After protein concentration analyzing, proteins were filled in the cell lysis buffer. Subsequently, the reaction buffer and DEVD-pNA substrate (caspase-3) were

supplemented into the lysis buffer. The reaction mixtures were cultured at 37℃ for 2 h. The absorbance at 405 nm was assessed via a microplate reader (Meigu, Shanghai, China).

ELISA

ELISA was performed by applying the ELISA kits for TNF-α and IL-1β (Abcam Biotechnology, USA) in order to detect the concentration of TNF-α and IL-1β in culture supernatant of TC-1 and WI-38 cells, Absorbance at 450 nm was determined via a microplate reader according to manufacturer's protocols

Statistical analysis

Data were presented as means± SD. The differences between or among groups were evaluated by Student's test or one-way analysis of variance (ANOVA). *P* value less than 0.05 was considered significant. All experiments were done at least three times.

Results

TLR4 was upregulated in ALI mice and LPS-induced cells

To investigate the potential role of TLR4 in lung injury, the ALI mice model was established via intratracheally instilling with LPS. Based on the observation via microscope, the intact alveolar structure without thickening or lymphocyte infiltration was observed in the lungs of sham-operated mice (left panel, Figure 1A). Nevertheless, it could easily found the pulmonary lesions in ALI mice, and pathologically thickened alveolar walls, collapsed alveoli and infiltrated inflammatory cells could also observed in ALI mice (right panel, Figure 1A), suggesting our ALI mice model was successfully constructed. Further, RT-qPCR and western blot were conducted to respectively investigate the mRNA and protein expression of TLR4. The data revealed that TLR4 was prominently upregulated in lung tissues of ALI mice and LPS-induced WI-38 cells (Figure 1B-D). The results above demonstrated that TLR4 was highly expressed in ALI mice and LPS-induced WI-38 cells.

TLR4 was a direct target of miR-26a-5p

It is reported that miRNAs widely participate in the regulation of biological processes through targeting the 3' untranslated region of the target mRNA(s) (Bushati & Cohen, 2007). In order to find out the potential miRNAs might bind with TLR4, we searched RNA22v2 database online websites and found the underlying binding sites between miR-26a-5p and TLR4 of human and mouse (Figure 2A). Next, miR-26a-5p expression was elevated through transfection with miR-26a-5p mimics and reduced via transfection with anti-miR-26a-5p in WI-38 and TC-1 cells according to RT-qPCR analysis (Figure 2B). For verifying the relationship between miR-26a-5p and TLR4, luciferase assay was then carried out. The result disclosed that the luciferase activity of pmirGLO-TLR4-WT was overtly decreased by miR-26a-5p mimics but increased by miR-26a-5p inhibitor, while the luciferase activity of pmirGLO-TLR4-Mut had no distinct change (Figure 2C-D). These findings suggested that miR-26a-5p could bind with TLR4. Moreover, RT-qPCR and western blot analyses demonstrated that the TLR4 mRNA and protein levels were declined in

the miR-26a-5p mimics group but increased in miR-26a-5p inhibitor group after lung injury (Figure 2E-F). Furthermore, miR-26a-5p level was remarkably decreased in ALI mice and LPS-induced WI-38 cell (Figure 2G-H). Altogether, miR-26a-5p could directly bind with TLR4.

MiR-26a-5p overexpression blocked the production of inflammatory factors via targeting TLR4

Then, we explored whether miR-26a-5p influenced lung injury and inflammation by targeting TLR4. To begin with, TLR4 expression was effectively increased by AAV-TLR4 injection (Figure 3A). H&E staining miR-26a-5p overexpression alleviated the lung injury in ALI mice, while this effect was reversed by TLR4 upregulation (Figure 3B-C). Moreover, we identified that miR-26a-5p overexpression reduced the lung drying wet ratio, but upregulation of TLR4 abolished the effects (Figure 3C). Furthermore, miR-26a-5p overexpression downregulated the contents of TNF-α and IL-1β in ALI mice's serum, LPS-induced WI-38 and TC-1 cells supernatants, whereas TLR4 overexpression counteracted the effects (Figure 3E-G). Collectively, we draw a conclusion that miR-26a-5p overexpression alleviated lung injury and inhibited inflammatory response via targeting TRL4.

MiR-26a-5p overexpression reduced cell apoptosis by targeting TRL4

To probe whether the interaction of miR-26a-5p and TLR4 was involved in cell apoptosis in ALI, we detected cell apoptosis via flow cytometry assay and the levels of Bax, Bcl-2 and caspase-3. As found in the results, miR-26a-5p overexpression downregulated Bax expression but increased Bcl-2 expression in ALI mice while TLR4 upregulation reversed the effects. (Figure 4A). Moreover, the decreased activity of caspase-3 in ALI mice by elevation of miR-26a-5p was reversed by TLR4 overexpression (Figure 4B). Furthermore, miR-26a-5p overexpression reduced cell apoptosis but TLR4 upregulation counteracted the effect in TC-1 and WI-38 cells (Figure 4C). Besides, the level of Bax was decreased while the level of Bcl-2 was upregulated by overexpression of miR-26a-5p in LPS-treated TC-1 and WI-38 cells, while TRL4 upregulation inversely changed these effects (Figure 4D-E). As presented in Figure 4F, miR-26a-5p overexpression decreased the caspase-3 activity in TC-1 and WI-38 cells, and TLR4 upregulation abolished the effect. Collectively, above findings indicated that miR-26a-5p overexpression could reduce cell apoptosis through targeting TLR4.

OIP5-AS1 could bind with miR-26a-5p

As some reports show that lncRNAs can serve as a sponge of miRNA to regulate the development of diseases (J. Fan, Zhang, Huang, & Li, 2019; Ouyang, Zhang, Tang, & Wang, 2019; Yu et al., 2019). We suspected there might be such a lncRNA that could bind with miR-26a-5p to affect the progression of ALI. According to starBase website (http://starbase.sysu.edu.cn), total 28 lncRNAs were screened out for further exploration (condition: high stringency of CLIP Data; supplementary table 1). These lncRNAs expression was determined by RT-qPCR and shown in Figure 5A. The heatmap displayed that only OIP5-AS1 was upregulated in lung tissues from ALI group while the rest lncRNA indicated no differentiated expression. We used starBase website and found the potential binding sites between OIP5-AS1 and miR-26a-5p (Figure 5B). To validate the relationship between OIP5-AS1 and miR-26a-5p, luciferase reporter

and RIP assay were conducted in WI-38 and TC-1 cells. Luciferase reporter assay showed that luciferase activity of pmirGLO-OIP5-AS1-WT was prominently decreased in miR-26a-5p transfected cells but increased in anti-miR-26a-5p transfected cells, while no significant change was detected in pGLO-OIP5-AS1-Mut group (Figure 5C). RIP assay indicated that OIP5-AS1 and miR-26a-5p were enriched in Ago2 groups but not in IgG groups (Figure 5D-E). All these results illustrated that OIP5-AS1 could bind with miR-26a-5p. Then, we identified that miR-26a-5p overexpression led to a prominent decline of OIP5-AS1 expression, and miR-26a-5p downregulation resulted in an increase of OIP5-AS1 expression (Figure 5F), suggesting that OIP5-AS1 could negatively regulated by miR-26a-5p. Thereafter, the data from RT-qPCR discovered OIP5-AS1 was upregulated in ALI mice and WI-38 cells (Figure 5G-H). To sum up, OIP5-AS1 could bind with miR-26a-5p in ALI.

OIP5-AS1 accelerated the production of inflammatory factors by sponging miR-26a-5p

To determine whether OIP5-AS1/miR-26a-5p axis could exert function in ALI, rescue assays were conducted. H&E staining showed miR-26a-5p upregulation alleviated OIP5-AS1 overexpression mediated the lung injury in ALI mice (Figure 6A-B). The lung drying wet ratio was increased after OIP5-AS1 upregulation, while miR-26a-5p overexpression abrogated the effect (Figure 6C). Moreover, OIP5-AS1 upregulation enhanced the mRNA levels of TNF-α and IL-1β, whereas miR-26a-5p overexpression significantly abrogated the effects in ALI mice, WI-38 and TC-1 cells (Figure 6D-F). These results suggested that OIP5-AS1 accelerated the production of inflammatory factor by sponging miR-26a-5p.

OIP5-AS1 facilitated cell apoptosis via sponging miR-26a-5p

Furthermore, we evaluated whether the OIP5-AS1/miR-26a-5p axis affected the apoptosis of TC-1 and WI-38 cells. We discovered that overexpression of miR-26a-5p reversed the effect of OIP5-AS1 upregulation on Bax and Bcl-2 protein levels (Figure 7A). Afterwards, ELISA analysis disclosed that miR-26a-5p overexpression abolished the promotive effect of OIP5-AS1 on caspase-3 activity (Figure 7B). Additionally, miR-26a-5p upregulation counteracted the aggravated influence of OIP5-AS1 on cell apoptosis in ALI mice (Figure 7C). The level of Bax was increased while the level of Bcl-2 was suppressed by OIP5-AS1 overexpression in TC-1 and WI-38 cells, and the result was recovered by the upregulation of miR-26a-5p (Figure 7D-E). As presented in Figure 7F, the caspase-3 activity was increased after LPS treatment in TC-1 and WI-38 cells, and further increased by OIP5-AS1 upregulation, but repressed by miR-26a-5p mimics. In conclusion, all the findings indicated that OIP5-AS1 promoted cell apoptosis via regulating miR-26a-5p.

Discussion

ALI is a severe illness that threats health and lives worldwide because of the high incidence and mortality (Ding, Pan, Wang, & Xu, 2016). TLR4, also known as TOLL (Engelmann et al., 2020), is a member of the Toll-like receptor family which plays a fundamental role in pathogen recognition and activation of innate immunity (Takizawa et al., 2017, 2020). Moreover, the toll-like receptors exhibit different patterns of expression and involve in LPS-induced signal transduction events in most gram-negative bacteria

(Kayagaki et al., 2013). Previous studies have proven that TLR4 displayed high level in ALI tissues and significantly facilitated the inflammatory response and cell apoptosis in ALI (Bachmaier et al., 2007; Tauseef et al., 2012). Similarly, the upregulation of TLR4 was also identified in ALI mice and LPS-induced WI-38 cells in our research.

We then further explored the upstream regulatory mechanism of TLR4. Considering TLR4 was reported to be inhibited by multiple miRNAs including miR-214 and miR-1178 (Lakhia et al., 2020; Wu et al., 2020), we then predicted the potential miRNA that could bind with TLR4, and miR-26a-5p was confirmed to directly target TLR4 in TC-1 and WI-38 cells. Moreover, miR-26a-5p negatively regulated TLR4. More importantly, miR-26a-5p overexpression inhibited the effects of TLR4 on inflammatory response and cell apoptosis. In summary, miR-26a-5p could regulate the development of ALI via targeting TLR4.

It is widely accepted that lncRNAs are able to act as miRNA “sponges” to competitively combining with miRNA to release target mRNA (Sen, Ghosal, Das, Balti, & Chakrabarti, 2014). In ALI, TUG1 was identified to alleviate sepsis-induced inflammation and apoptosis via miR-34b-5p/GAB1 axis (Qiu, Xu, & He, 2020). Besides, downregulated CASC9 aggravates cell apoptosis through miR-195-5p/PDK4 axis (Wang, Guo, Liu, & Song, 2020). In our study, we confirmed that OIP5-AS1 could bind with miR-26a-5p by using RNA immunoprecipitation (RIP) and luciferase reporter assay. Previously, OIP5-AS1 was reported to exert different effects on cell injury and inflammatory response in different pathogenesis. In arheumatoid arthritis, OIP5-AS1 was proposed to inhibit inflammation response via blocking TLR3- NF-κB pathway (Qing & Liu, 2020). In atherosclerosis, OIP5-AS1 was confirmed to facilitate cell apoptosis and inflammation by activating AKT/NF-κB pathway (Ren et al., 2020). In current study, we identified that miR-26a-5p negatively regulated the expression of OIP5-AS1. Additionally, OIP5-AS1 upregulation increased the lung injury scores, the lung wet/dry weight ratio, proinflammatory factors production and cell apoptosis in ALI, miR-26a-5p elevation counteracted these effects.

In summary, our results proved that OIP5-AS1 aggravated ALI through promoting inflammation and cell apoptosis by regulating miR-26a-5p/TLR4 axis, which offers new insights into the therapeutic strategy.

Declarations

Ethics approval and consent to participate

All experimental procedures were based on the National Institutes of Health Guidelines for the Care and Use of Laboratory Animals and approved by the Ethics Committee of The Affiliated Huaian No.1 People's Hospital of Nanjing Medical University. All methods were conducted in accordance with the ARRIVE guidelines (https://arriveguidelines.org).

Consent for publication

Not applicable

Acknowledgement

We thank all participators for their help.

Conflicts of interest

None.

Availability of data and materials

The datasets used and/or analysed during the current study available from the corresponding author on reasonable request.

Funding

None

Authors' contributions

Qingsong Sun and Man Luo conceived and designed the experiments. Qingsong Sun, Man Luo, Zhiwei Gao, Xiang Han, Weiqin Wu, and Hongmei Zhao carried out the experiments. Qingsong Sun, Man Luo, and Hongmei Zhao analyzed the data. Qingsong Sun, Man Luo, and Hongmei Zhao drafted the manuscript. All authors agreed to be accountable for all aspects of the work. All authors have read and approved the final manuscript.

References

Abdollahzadeh, R., Daraei, A., Mansoori, Y., Sepahvand, M., Amoli, M. M., & Tavakkoly-Bazzaz, J. (2019). Competing endogenous RNA (ceRNA) cross talk and language in ceRNA regulatory networks: A new look at hallmarks of breast cancer. *J Cell Physiol, 234*(7), 10080-10100. doi:10.1002/jcp.27941

Ali, F. F., Abdel-Hamid, H. A., & Toni, N. D. (2018). H2S attenuates acute lung inflammation induced by administration of lipopolysaccharide in adult male rats. *Gen Physiol Biophys*. doi:10.4149/gpb_2018002

Bachmaier, K., Toya, S., Gao, X., Triantafillou, T., Garrean, S., Park, G. Y., . . . Malik, A. B. (2007). E3 ubiquitin ligase Cblb regulates the acute inflammatory response underlying lung injury. *Nat Med, 13*(8), 920-926. doi:10.1038/nm1607

Bartel, D. P. (2004). MicroRNAs: genomics, biogenesis, mechanism, and function. *Cell, 116*(2), 281-297. doi:10.1016/s0092-8674(04)00045-5

Bushati, N., & Cohen, S. M. (2007). microRNA functions. *Annu Rev Cell Dev Biol, 23*, 175-205. doi:10.1146/annurev.cellbio.23.090506.123406

Chen, X., Xiong, D., Yang, H., Ye, L., Mei, S., Wu, J., . . . Huang, L. (2019). Long noncoding RNA OPA-interacting protein 5 antisense transcript 1 upregulated SMAD3 expression to contribute to metastasis of cervical cancer by sponging miR-143-3p. *J Cell Physiol, 234*(4), 5264-5275. doi:10.1002/jcp.27336

Ding, X. M., Pan, L., Wang, Y., & Xu, Q. Z. (2016). Baicalin exerts protective effects against lipopolysaccharide-induced acute lung injury by regulating the crosstalk between the CX3CL1-CX3CR1 axis and NF-kappaB pathway in CX3CL1-knockout mice. *Int J Mol Med, 37*(3), 703-715. doi:10.3892/ijmm.2016.2456

Engelmann, C., Sheikh, M., Sharma, S., Kondo, T., Loeffler-Wirth, H., Zheng, Y. B., . . . Jalan, R. (2020). Toll-like receptor 4 is a therapeutic target for prevention and treatment of liver failure. *J Hepatol, 73*(1), 102-112. doi:10.1016/j.jhep.2020.01.011

Fan, J., Zhang, J., Huang, S., & Li, P. (2019). lncRNA OSER1-AS1 acts as a ceRNA to promote tumorigenesis in hepatocellular carcinoma by regulating miR-372-3p/Rab23 axis. *Biochem Biophys Res Commun*. doi:10.1016/j.bbrc.2019.10.105

Fan, J. L., Zhang, L., & Bo, X. H. (2020). MiR-126 on mice with coronary artery disease by targeting S1PR2. *Eur Rev Med Pharmacol Sci, 24*(2), 893-904. doi:10.26355/eurrev_202001_20074

Favarin, D. C., de Oliveira, J. R., de Oliveira, C. J., & Rogerio Ade, P. (2013). Potential effects of medicinal plants and secondary metabolites on acute lung injury. *Biomed Res Int, 2013*, 576479. doi:10.1155/2013/576479

Gonzalez-Guerrero, C., Cannata-Ortiz, P., Guerri, C., Egido, J., Ortiz, A., & Ramos, A. M. (2017). TLR4-mediated inflammation is a key pathogenic event leading to kidney damage and fibrosis in cyclosporine nephrotoxicity. *Arch Toxicol, 91*(4), 1925-1939. doi:10.1007/s00204-016-1830-8

Guo, R. F., & Ward, P. A. (2007). Role of oxidants in lung injury during sepsis. *Antioxid Redox Signal, 9*(11), 1991-2002. doi:10.1089/ars.2007.1785

Ho, M. S., Mei, S. H., & Stewart, D. J. (2015). The Immunomodulatory and Therapeutic Effects of Mesenchymal Stromal Cells for Acute Lung Injury and Sepsis. *J Cell Physiol, 230*(11), 2606-2617. doi:10.1002/jcp.25028

Hu, L., Yang, H., & Ai, M. (2017). Inhibition of TLR4 alleviates the inflammation and apoptosis of retinal ganglion cells in high glucose. *255*(11), 2199-2210. doi:10.1007/s00417-017-3772-0

Jiang, Y., Zhu, F., Wu, G. S., Wang, K. A., Wang, C., Yu, Q., . . . Xia, Z. F. (2020). Microarray and bioinformatics analysis of circular RNAs expression profile in traumatic lung injury. *Exp Ther Med, 20*(1), 227-234. doi:10.3892/etm.2020.8686

Kayagaki, N., Wong, M. T., Stowe, I. B., Ramani, S. R., Gonzalez, L. C., Akashi-Takamura, S., . . . Dixit, V. M. (2013). Noncanonical inflammasome activation by intracellular LPS independent of TLR4. *Science, 341*(6151), 1246-1249. doi:10.1126/science.1240248

Lakhia, R., Yheskel, M., Flaten, A., Ramalingam, H., Aboudehen, K., Ferrè, S., . . . Patel, V. (2020). Interstitial microRNA miR-214 attenuates inflammation and polycystic kidney disease progression. *JCI Insight, 5*(7).

doi:10.1172/jci.insight.133785

Li, H., Shi, H., Gao, M., Ma, N., & Sun, R. (2018). Long non-coding RNA CASC2 improved acute lung injury by regulating miR-144-3p/AQP1 axis to reduce lung epithelial cell apoptosis. *Cell Biosci, 8*, 15. doi:10.1186/s13578-018-0205-7

Li, Y., Huang, J., Yan, H., Li, X., Ding, C., Wang, Q., & Lu, Z. (2020). Protective effect of microRNA381 against inflammatory damage of endothelial cells during coronary heart disease by targeting CXCR4. *Mol Med Rep*. doi:10.3892/mmr.2020.10957

Lou, J., Hu, Y., Wu, M. D., Che, L. Q., Wu, Y. F., Zhao, Y., . . . Shen, H. H. (2019). Endothelial cell-specific anticoagulation reduces inflammation in a mouse model of acute lung injury. *Acta Pharmacol Sin, 40*(6), 769-780. doi:10.1038/s41401-018-0175-7

Lou, W., Ding, B., & Fu, P. (2020). Pseudogene-Derived lncRNAs and Their miRNA Sponging Mechanism in Human Cancer. *Front Cell Dev Biol, 8*, 85. doi:10.3389/fcell.2020.00085

Ma, Y. S., Chu, K. J., Ling, C. C., Wu, T. M., Zhu, X. C., Liu, J. B., . . . Zhang, X. W. (2020). Long Noncoding RNA OIP5-AS1 Promotes the Progression of Liver Hepatocellular Carcinoma via Regulating the hsa-miR-26a-3p/EPHA2 Axis. *Mol Ther Nucleic Acids, 21*, 229-241. doi:10.1016/j.omtn.2020.05.032

Machackova, T., Mlcochova, H., Stanik, M., Dolezel, J., Fedorko, M., Pacik, D., . . . Slaby, O. (2016). MiR-429 is linked to metastasis and poor prognosis in renal cell carcinoma by affecting epithelial-mesenchymal transition. *Tumour Biol, 37*(11), 14653-14658. doi:10.1007/s13277-016-5310-9

Mahadeo, K. M., Bajwa, R., Abdel-Azim, H., Lehmann, L. E., Duncan, C., Zantek, N., . . . Corbacioglu, S. (2020). Diagnosis, grading, and treatment recommendations for children, adolescents, and young adults with sinusoidal obstructive syndrome: an international expert position statement. *Lancet Haematol, 7*(1), e61-e72. doi:10.1016/s2352-3026(19)30201-7

Niu, X., Pu, S., Ling, C., Xu, J., Wang, J., Sun, S., . . . Zhang, Z. (2020). lncRNA Oip5-as1 attenuates myocardial ischaemia/reperfusion injury by sponging miR-29a to activate the SIRT1/AMPK/PGC1α pathway. *Cell Prolif, 53*(6), e12818. doi:10.1111/cpr.12818

Ouyang, T., Zhang, Y., Tang, S., & Wang, Y. (2019). Long non-coding RNA LINC00052 regulates miR-608/EGFR axis to promote progression of head and neck squamous cell carcinoma. *Exp Mol Pathol*, 104321. doi:10.1016/j.yexmp.2019.104321

Qing, P., & Liu, Y. (2020). Inhibitory role of long non-coding RNA OIP5-AS1 in rheumatoid arthritis progression through the microRNA-448-paraoxonase 1-toll-like receptor 3-nuclear factor κB axis. *Exp Physiol*. doi:10.1113/ep088608

Qiu, N., Xu, X., & He, Y. (2020). LncRNA TUG1 alleviates sepsis-induced acute lung injury by targeting miR-34b-5p/GAB1. *BMC Pulm Med, 20*(1), 49. doi:10.1186/s12890-020-1084-3

Ren, M., Wang, T., Han, Z., Fu, P., Liu, Z., & Ouyang, C. (2020). LncRNA OIP5-AS1 contributes to the progression of atherosclerosis by targeting miR-26a-5p through AKT/NF-κB pathway. *J Cardiovasc Pharmacol*. doi:10.1097/fjc.0000000000000889

Rieger, A. M., Nelson, K. L., Konowalchuk, J. D., & Barreda, D. R. (2011). Modified annexin V/propidium iodide apoptosis assay for accurate assessment of cell death. *J Vis Exp*(50). doi:10.3791/2597

Sadowitz, B., Roy, S., Gatto, L. A., Habashi, N., & Nieman, G. (2011). Lung injury induced by sepsis: lessons learned from large animal models and future directions for treatment. *Expert Rev Anti Infect Ther, 9*(12), 1169-1178. doi:10.1586/eri.11.141

Sen, R., Ghosal, S., Das, S., Balti, S., & Chakrabarti, J. (2014). Competing endogenous RNA: the key to posttranscriptional regulation. *ScientificWorldJournal, 2014*, 896206. doi:10.1155/2014/896206

Shin, N. R., Park, S. H., Ko, J. W., Ryu, H. W., Jeong, S. H., Kim, J. C., . . . Shin, I. S. (2017). Artemisia argyi attenuates airway inflammation in lipopolysaccharide induced acute lung injury model. *Lab Anim Res, 33*(3), 209-215. doi:10.5625/lar.2017.33.3.209

Song, C., Li, H., Li, Y., Dai, M., Zhang, L., Liu, S., . . . Pan, P. (2019). NETs promote ALI/ARDS inflammation by regulating alveolar macrophage polarization. *Exp Cell Res, 382*(2), 111486. doi:10.1016/j.yexcr.2019.06.031

Takizawa, H., Fritsch, K., Kovtonyuk, L. V., Saito, Y., Yakkala, C., Jacobs, K., . . . Manz, M. G. (2017). Pathogen-Induced TLR4-TRIF Innate Immune Signaling in Hematopoietic Stem Cells Promotes Proliferation but Reduces Competitive Fitness. *Cell Stem Cell, 21*(2), 225-240.e225. doi:10.1016/j.stem.2017.06.013

Takizawa, H., Fritsch, K., Kovtonyuk, L. V., Saito, Y., Yakkala, C., Jacobs, K., . . . Manz, M. G. (2020). Pathogen-Induced TLR4-TRIF Innate Immune Signaling in Hematopoietic Stem Cells Promotes Proliferation but Reduces Competitive Fitness. *Cell Stem Cell, 27*(1), 177. doi:10.1016/j.stem.2020.06.010

Tauseef, M., Knezevic, N., Chava, K. R., Smith, M., Sukriti, S., Gianaris, N., . . . Mehta, D. (2012). TLR4 activation of TRPC6-dependent calcium signaling mediates endotoxin-induced lung vascular permeability and inflammation. *J Exp Med, 209*(11), 1953-1968. doi:10.1084/jem.20111355

Vishnubalaji, R., Shaath, H., Elango, R., & Alajez, N. M. (2020). Noncoding RNAs as potential mediators of resistance to cancer immunotherapy. *Semin Cancer Biol, 65*, 65-79. doi:10.1016/j.semcancer.2019.11.006

Wang, H. R., Guo, X. Y., Liu, X. Y., & Song, X. (2020). Down-regulation of lncRNA CASC9 aggravates sepsis-induced acute lung injury by regulating miR-195-5p/PDK4 axis. *Inflamm Res, 69*(6), 559-568. doi:10.1007/s00011-020-01316-2

Wu, G., Zhou, W., Lin, X., Sun, Y., Li, J., Xu, H., . . . Tian, X. (2020). circRASSF2 Acts as ceRNA and Promotes Papillary Thyroid Carcinoma Progression through miR-1178/TLR4 Signaling Pathway. *Mol Ther Nucleic*

Acids, 19, 1153-1163. doi:10.1016/j.omtn.2019.11.037

Yu, P. F., Wang, Y., Lv, W., Kou, D., Hu, H. L., Guo, S. S., & Zhao, Y. J. (2019). LncRNA NEAT1/miR-1224/KLF3 contributes to cell proliferation, apoptosis and invasion in lung cancer. *Eur Rev Med Pharmacol Sci, 23*(19), 8403-8410. doi:10.26355/eurrev_201910_19151

Zhang, W., Chen, L., Jiang, Y., & Shen, Y. (2018). miR-26a-5p Regulates Synovial Fibroblast Invasion in Patients with Rheumatoid Arthritis by Targeting Smad 1. *Med Sci Monit, 24*, 5178-5184. doi:10.12659/msm.907816

Zhang, X. Z., Liu, H., & Chen, S. R. (2020). Mechanisms of Long Non-Coding RNAs in Cancers and Their Dynamic Regulations. *Cancers (Basel), 12*(5). doi:10.3390/cancers12051245

Zhang, Y., Su, Z., Liu, H. L., Li, L., Wei, M., Ge, D. J., & Zhang, Z. J. (2018). Effects of miR-26a-5p on neuropathic pain development by targeting MAPK6 in in CCI rat models. *Biomed Pharmacother, 107*, 644-649. doi:10.1016/j.biopha.2018.08.005

Zhang, Y., Zhu, Y., Gao, G., & Zhou, Z. (2019). Knockdown XIST alleviates LPS-induced WI-38 cell apoptosis and inflammation injury via targeting miR-370-3p/TLR4 in acute pneumonia. *Cell Biochem Funct, 37*(5), 348-358. doi:10.1002/cbf.3392

Zhao, Z., Sun, W., Guo, Z., Zhang, J., Yu, H., & Liu, B. (2020). Mechanisms of lncRNA/microRNA interactions in angiogenesis. *Life Sci, 254*, 116900. doi:10.1016/j.lfs.2019.116900

Zhi, L., Zhao, J., Zhao, H., Qing, Z., Liu, H., & Ma, J. (2020). Downregulation of LncRNA OIP5-AS1 Induced by IL-1β Aggravates Osteoarthritis via Regulating miR-29b-3p/PGRN. *Cartilage*, 1947603519900801. doi:10.1177/1947603519900801

Zhou, Z., Zhu, Y., Gao, G., & Zhang, Y. (2019). Long noncoding RNA SNHG16 targets miR-146a-5p/CCL5 to regulate LPS-induced WI-38 cell apoptosis and inflammation in acute pneumonia. *Life Sci, 228*, 189-197. doi:10.1016/j.lfs.2019.05.008

Zuniga, M. C., Raghuraman, G., Hitchner, E., Weyand, C., Robinson, W., & Zhou, W. (2017). PKC-epsilon and TLR4 synergistically regulate resistin-mediated inflammation in human macrophages. *Atherosclerosis, 259*, 51-59. doi:10.1016/j.atherosclerosis.2017.02.021

Zusso, M., Lunardi, V., Franceschini, D., Pagetta, A., Lo, R., Stifani, S., . . . Moro, S. (2019). Ciprofloxacin and levofloxacin attenuate microglia inflammatory response via TLR4/NF-kB pathway. *J Neuroinflammation, 16*(1), 148. doi:10.1186/s12974-019-1538-9

Figures

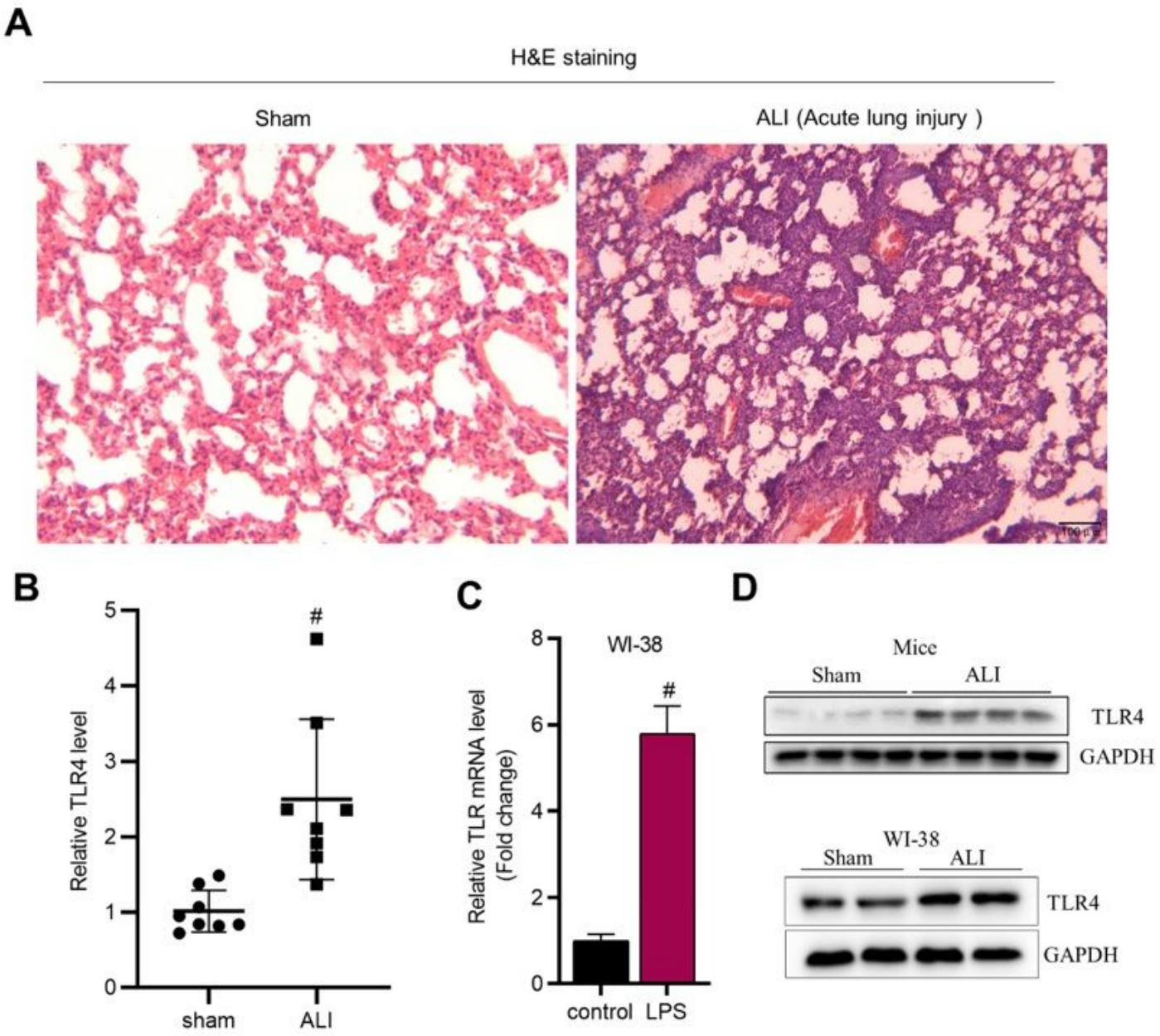

Figure 1

TLR4 was upregulated in ALI mice and LPS-induced cells. A, H&E staining was conducted to assess the lung injury degree in ALI mice. B-D, The mRNA and protein expression of TLR4 in mice's lung tissues (n=8 per group) and LPS-induced cells were respectively proved by RT-qPCR and western blot assay. #P< 0.05 compared with Sham group in B; #P< 0.05 compared with control group in C.

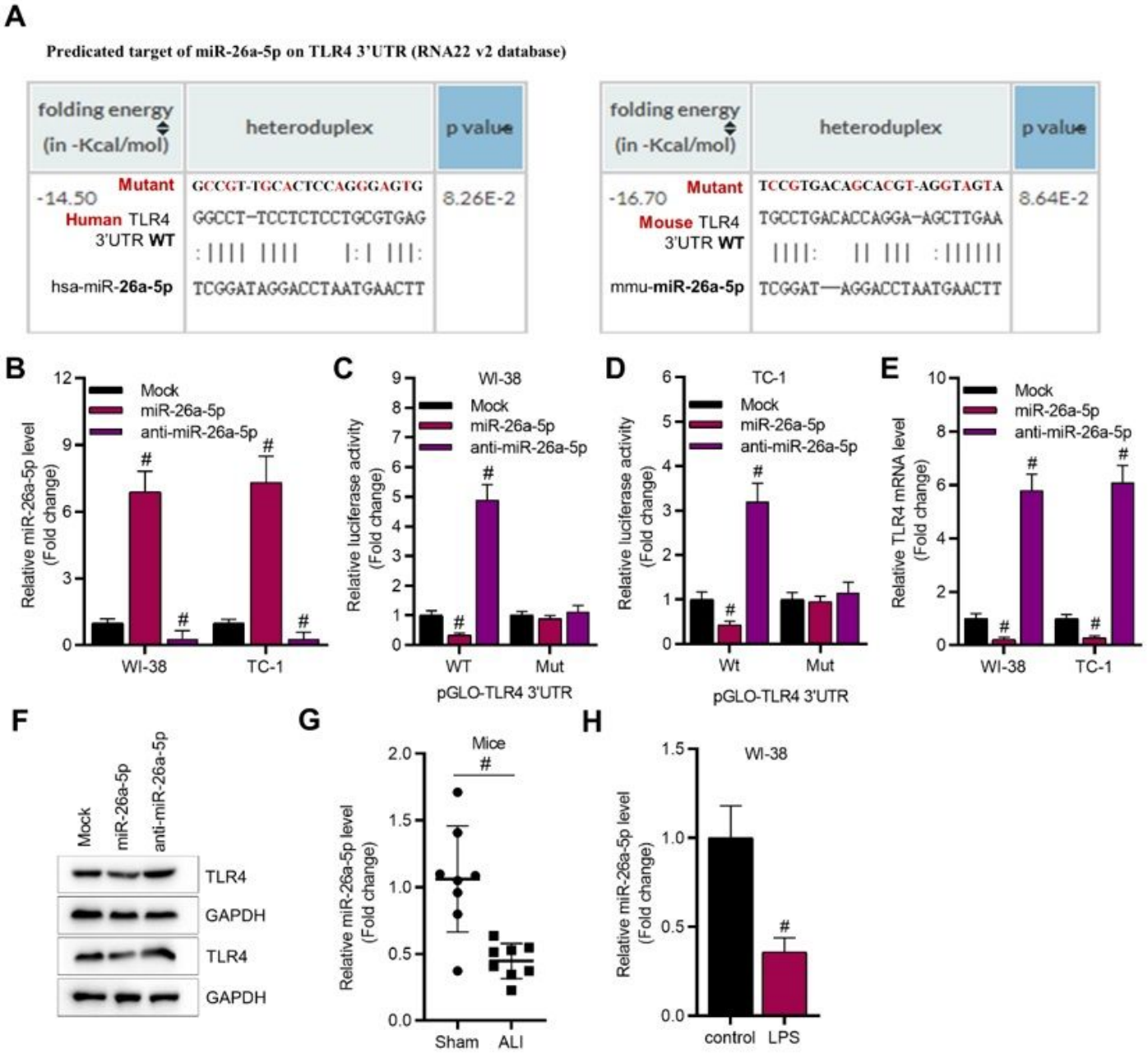

Figure 2

TLR4 could bind with miR-26a-5p. A, RNA22v2 database predicted the target of miR-26a-5p on TLR4. B, RT-qPCR assay was conducted to assess the efficiency of miR-26a-5p overexpression and miR-26a-5p knockdown in LPS-induced cells. C-D, Luciferase reporter assay was performed to verify the interaction between miR-26a-5p and TLR4. E-F, RT-qPCR and western blot assay were applied for detecting the effect of miR-26a-5p overexpression and miR-26a-5p knockdown to the mRNA and protein expression of TLR4 in WI-38 and TC-1 cells. G-H The expression of miR-26a-5p in mice's lung tissues (n=8 per group) and LPS-treated WI-38 cells was assessed by RT-qPCR assay. #P< 0.05 compared with Mock group in B, C, D, E; #P< 0.05 compared with Sham group in G; #P< 0.05 compared with control group in H.

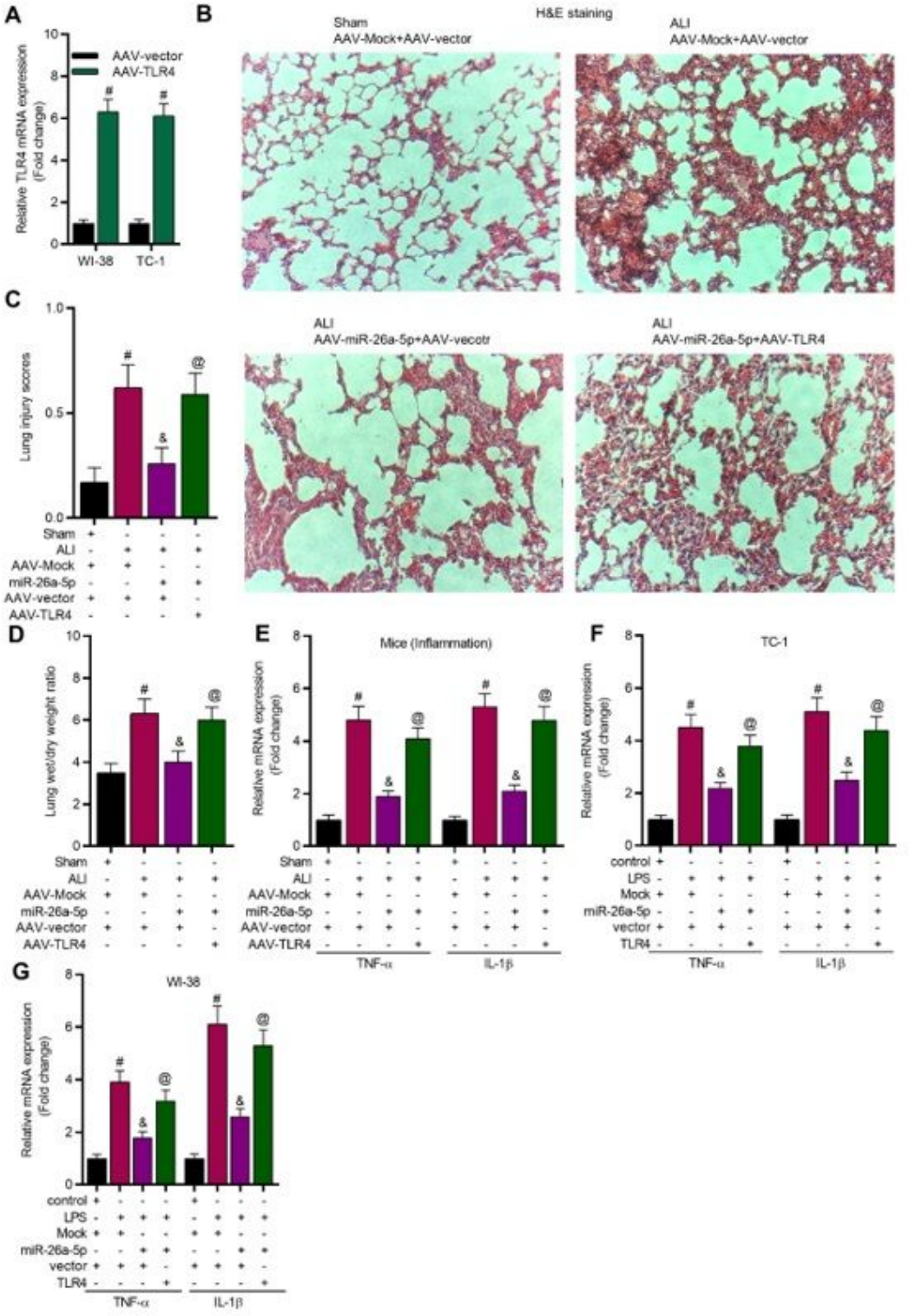

Figure 3

MiR-26a-5p inhibited the progression of lung injury by regulating TLR4. A, TLR4 expression was evaluated by RT-qPCR in mice's lung tissues (n=8 per group). B-C, H&E staining was conducted to assess the lung injury degree in mice's lung tissues (n=8 per group). D, Statistical analysis detected the lung wet/dry weight ratio in mice's lung tissues (n=8 per group). E-G, RT-qPCR was employed to evaluate the levels of TNF-α and IL-1β in mice's lung tissues (n=8 per group) as well as TC-1 and WI-38 cells. #P< 0.05

compared with AAV-vector group in A; #P< 0.05 compared with Sham + AAV-Mock + AAV-vector group, &P< 0.05 compared with ALI + AAV-Mock + AAV-vector group, @ P< 0.05 compared with ALI + AAV-miR-26a-5p + AAV-vector group in C, D, E; #P< 0.05 compared with control + Mock + vector group, &P< 0.05 compared with LPS + Mock + vector group, @ P< 0.05 compared with LPS + miR-26a-5p + vector group in F, G.

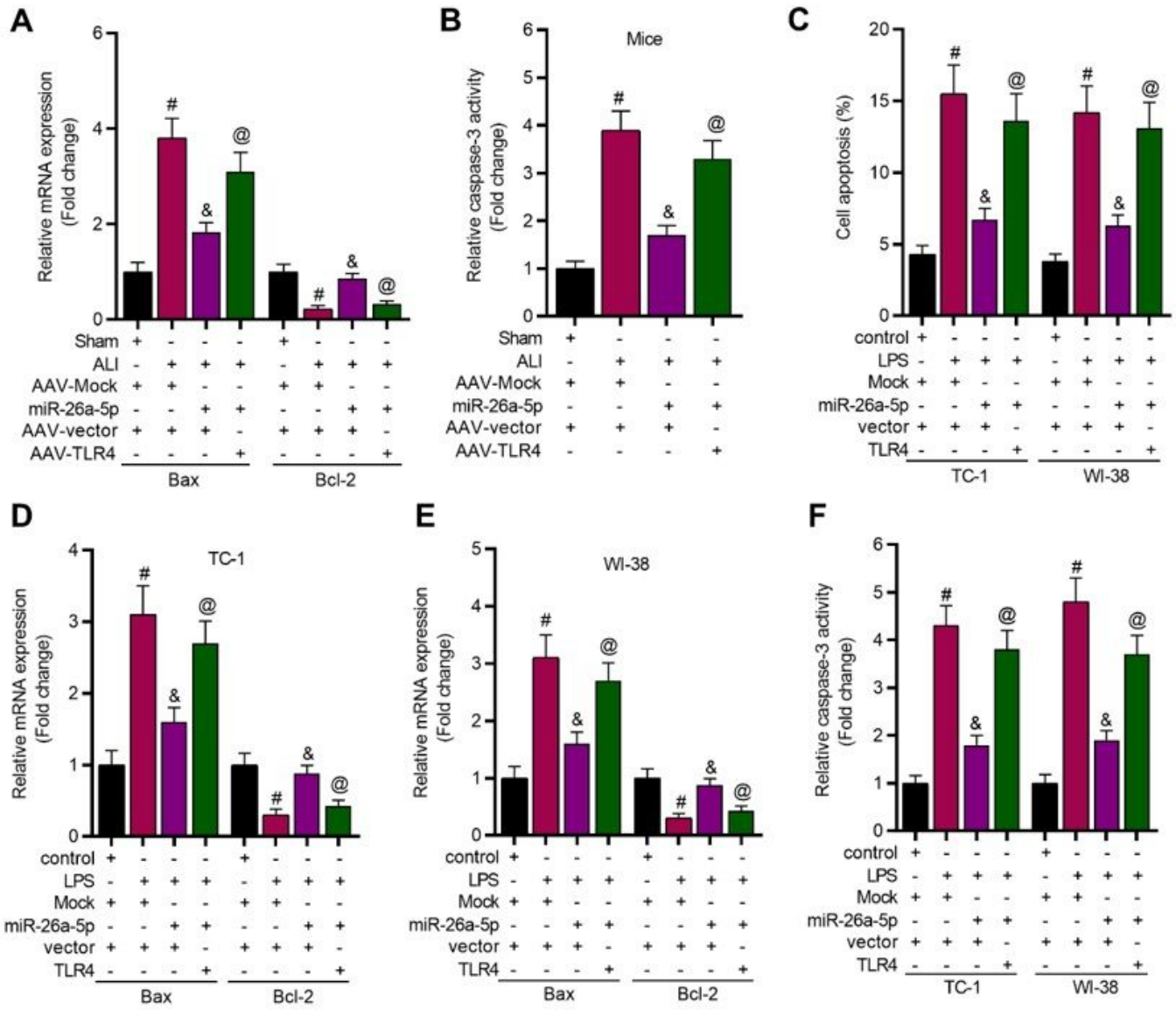

Figure 4

MiR-26a-5p overexpression alleviated cell apoptosis by modulating TLR4. A, RT-qPCR was conducted to detect Bax and Bcl-2 expression in mice's lung tissues (n=8 per group). B, The activity of caspase-3 in mice's lung tissues (n=8 per group) was determined. C, Flow cytometry assay was utilized to verify the percentage of cell apoptosis. D-E, Bax and Bcl-2 expression in cells was calculated by RT-qPCR. F, The activity of caspase-3 in cells was detect. #P< 0.05 compared with Sham + AAV-Mock + AAV-vector group, &P< 0.05 compared with ALI + AAV-Mock + AAV-vector group, @ P< 0.05 compared with ALI + AAV-miR-26a-5p + AAV-vector group in A, B, C; #P< 0.05 compared with control + Mock + vector group, &P< 0.05

compared with LPS + Mock + vector group, @ P< 0.05 compared with LPS + miR-26a-5p + vector group in D, E, F.

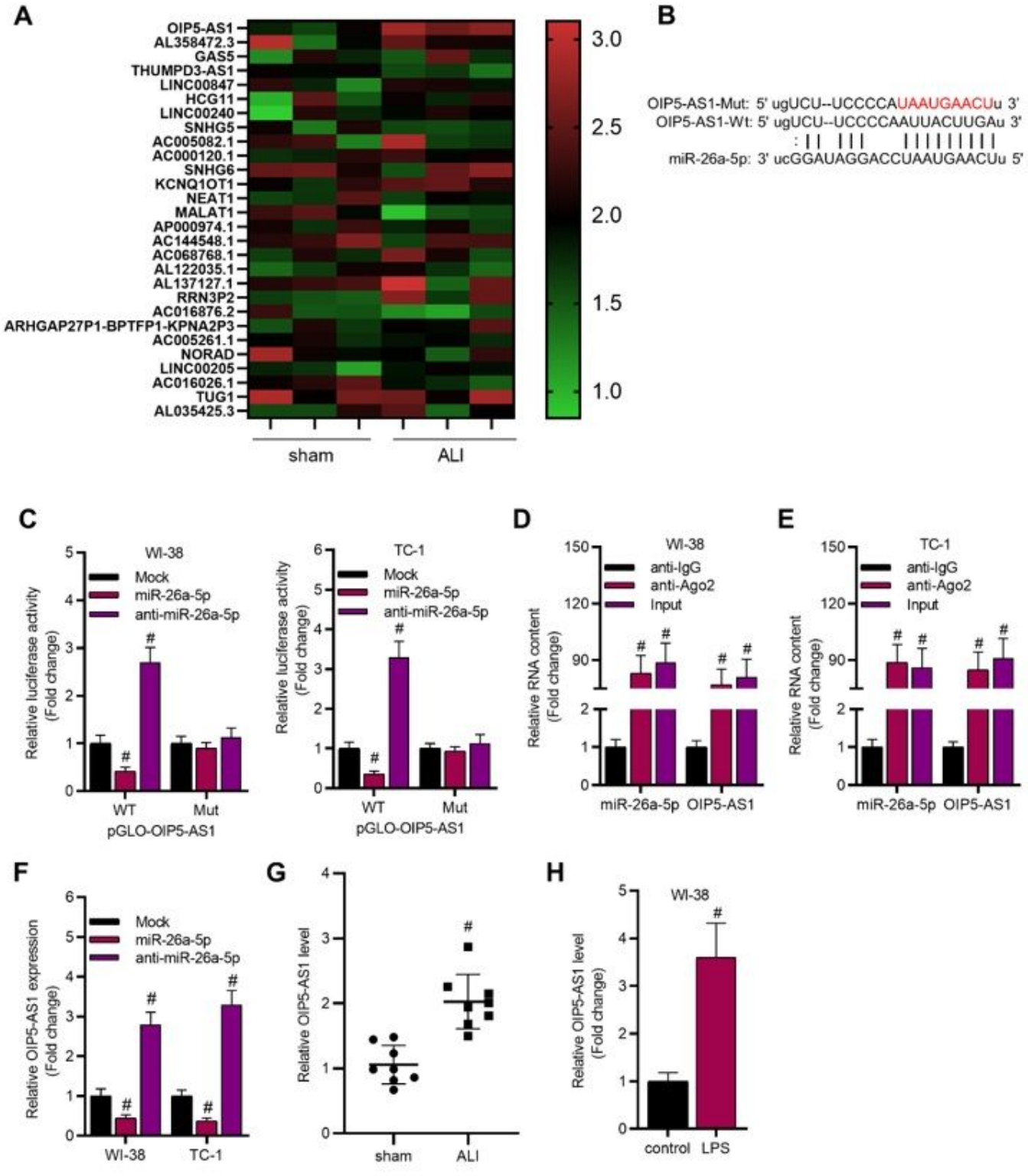

Figure 5

OIP5-AS1 regulated miR-26a-5p in ALI. A, The expression of predicted lncRNAs in lung tissues from sham and ALI groups. B, The predicted biding sites of miR-26a-5p on OIP5-AS1. C-E, The interaction between miR-26a-5p and OIP5-AS1 was demonstrated by luciferase reporter and RIP assays. F, The efficiency of

miR-26a-5p upregulation and miR-26a-5p knockdown on OIP5-AS1 expression were estimated by RT-qPCR. G-H, RT-qPCR assay was conducted to evaluate the level of OIP5-AS1 in mice's lung tissues (n=8 per group) and LPS-induced cells. #P< 0.05 compared with Mock group in B, C, F; #P< 0.05 compared with anti-IgG group in D, E; #P< 0.05 compared with Sham group in G; #P< 0.05 compared with control group in H.

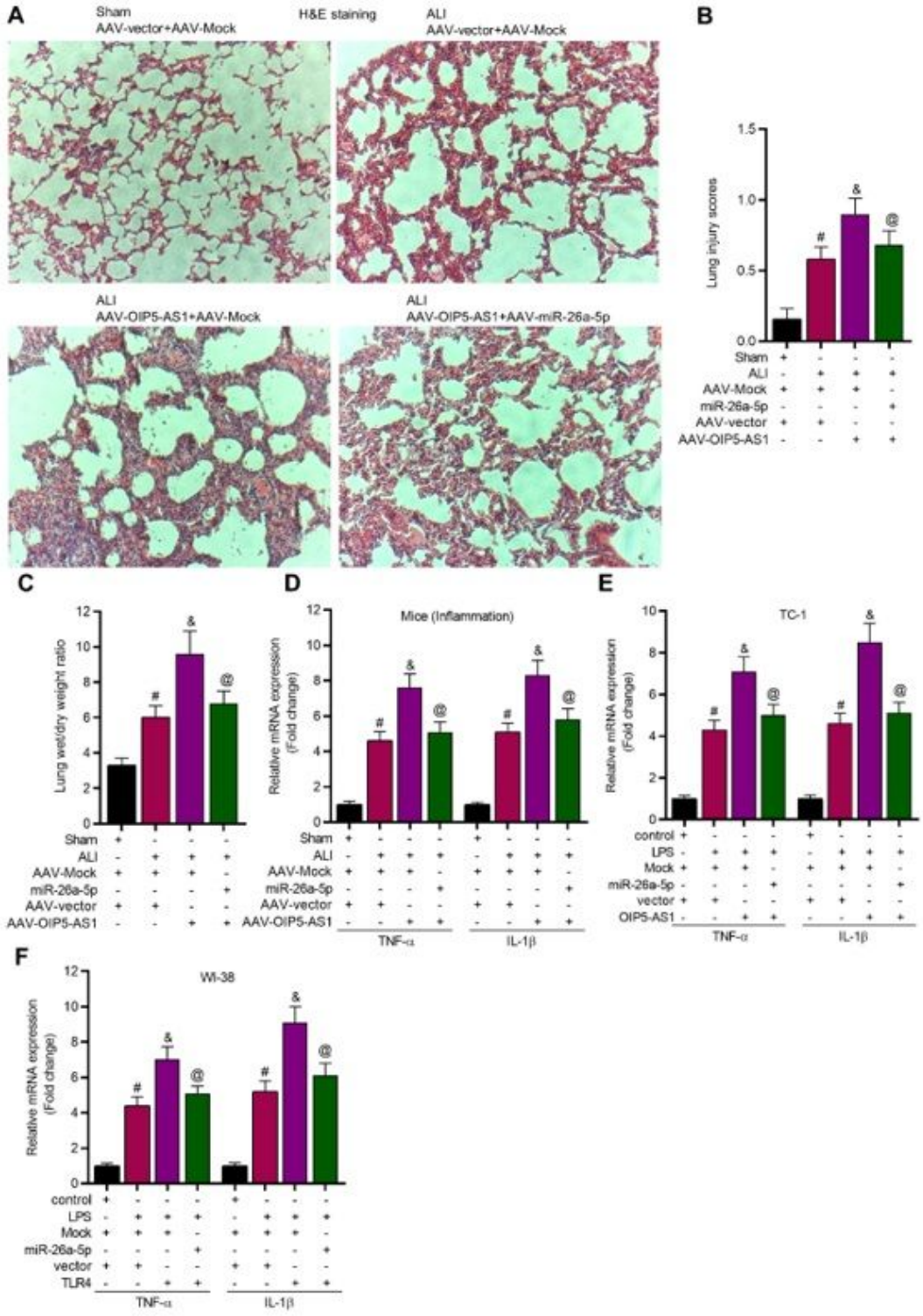

Figure 6

OIP5-AS1 promoted the inflammation injuries by targeting miR-26a-5p. A-B, H&E staining was carried out to detect the lung injury degree in ALI in mice's lung tissues (n=8 per group). C, Statistical analysis detected the lung wet/dry weight ratio (n=8 per group). D-F, RT-qPCR was applied to assess the levels of TNF-α and IL-1β in mice's serum (n=8 per group) and cell supernatant. #P< 0.05 compared with Sham + AAV-Mock + AAV-vector group, &P< 0.05 compared with ALI + AAV-Mock + AAV-vector group, @ P< 0.05 compared with ALI + AAV-miR-26a-5p + AAV-vector group in C, D; #P< 0.05 compared with control + Mock + vector group, &P< 0.05 compared with LPS + Mock + vector group, @ P< 0.05 compared with LPS + miR-26a-5p + vector group in E, F.

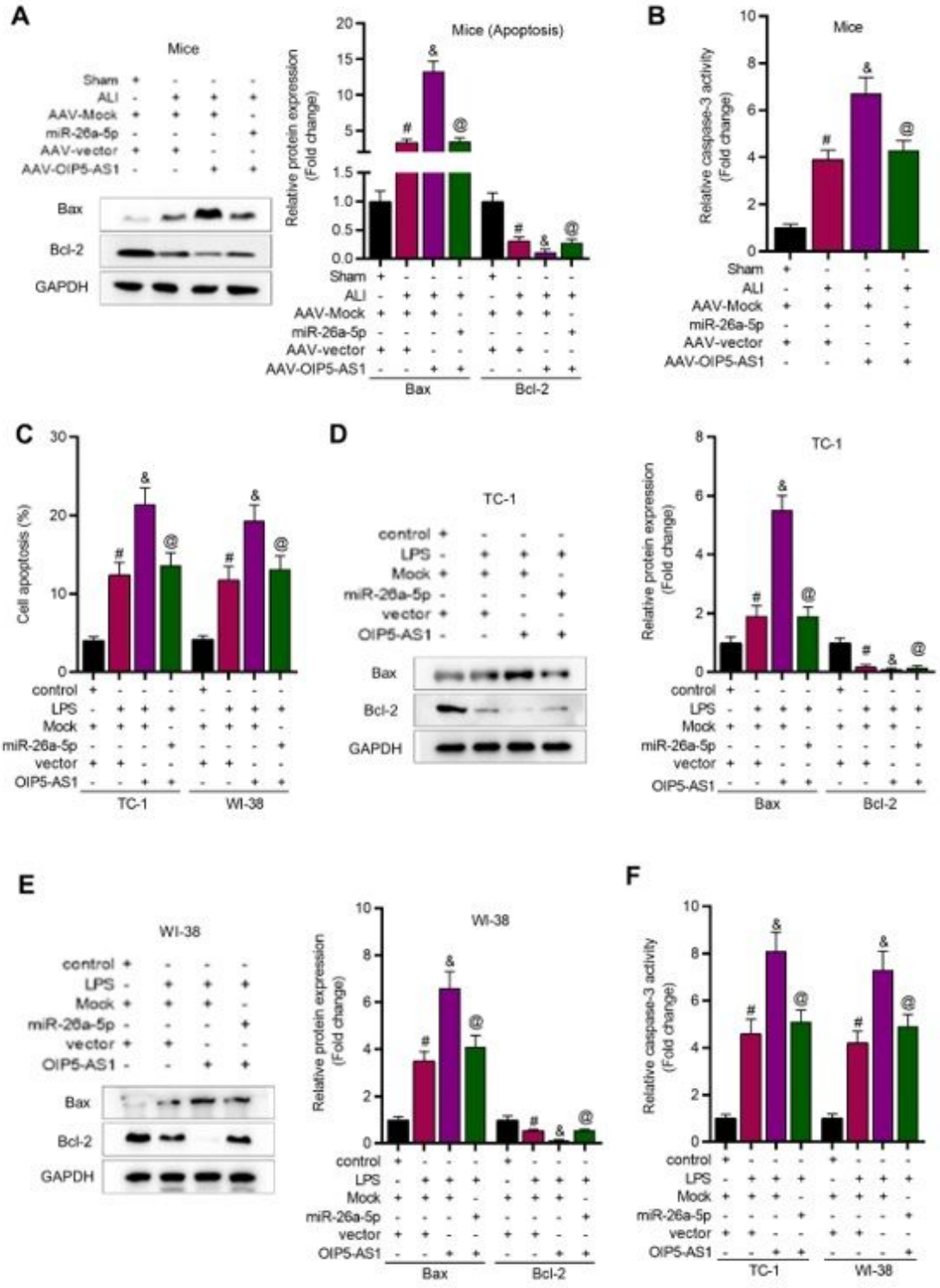

Figure 7

OIP5-AS1 accelerated cell apoptosis via regulating miR-26a-5p. A, The protein expression of apoptosis genes in ALI mice's lung tissues (n=8 per group) was assessed via western blot assay. B, ELISA was used to detect the activity of caspase-3 in ALI mice's lung tissues (n=8 per group). C, Flow cytometry assay was utilized to verify the percentage of cell apoptosis. D-E, The protein expression of apoptosis genes in cells was calculated by western blot assay. F, The activity of caspase-3 in cells was detected by ELISA. #P<

0.05 compared with Sham + AAV-Mock + AAV-vector group, &P< 0.05 compared with ALI + AAV-Mock + AAV-vector group, @ P< 0.05 compared with ALI + AAV-miR-26a-5p + AAV-vector group in A, B; #P< 0.05 compared with control + Mock + vector group, &P< 0.05 compared with LPS + Mock + vector group, @ P< 0.05 compared with LPS + miR-26a-5p + vector group in C, D, E, F.

Supplementary Files

This is a list of supplementary files associated with this preprint. Click to download.

- supplementarytable1.xls